Southern Horizons in Time-Domain Astronomy
Proceedings IAU Symposium No. 339, 2019
E. Griffin, ed.

doi:10.1017/S1743921318002752

Calibration and Standardisation

Workshop 14

C. Sterken

Department of Physics, University of Brussels, Brussels, Belgium
email: csterken@vub.ac.be

Abstract. One of the great challenges in time-domain astronomy is the problem of combining data obtained at various epochs with very different instruments. These problems are mostly discussed from within a specific observational mode, for example photometry, spectroscopy or imaging. This Workshop explored by example diverse pitfalls of time-domain calibration by discussing calibration and standardisation problems across various types of variables.

Keywords. Stars: imaging, stars: individual (AG Car, η Car, CY Aqr, HD 269209, HD 34664, Tr 16-64, Tr 16-65, HD 303308, CPD −59 2628), techniques: photometric

1. Introduction

Standardisation is the procedure of reducing the instrumental observables (magnitudes, colours, radial velocities, . . .) obtained in a specific system of mensuration to the standard set up by the designers of that system. (For the rules that are referred to in the case of the *UBV* system, see the paper by Sterken, p. 139). Standardisation is also the creation of specific data-reduction procedures to which one has to adhere, and includes the provision of standard stars that permit one to follow those procedures.

Transformation is the process of transforming instrumental data to a standard scale.

Calibration is the action that outlines which are the variables that may distort or spoil the instrumental data; it operates the procedures that control those variables, and quantifies their impact. In CCD imaging, the complete sequence of calibration steps leads to a calibrated image; bias and flat-field corrections are *only* the first steps of an incomplete calibration procedure, so a bias-corrected and flat-fielded image should thus never be called 'a calibrated image'.

Some observers call comparison stars 'standards', while others might observe their standards in non-standard conditions – for example, during twilight. We must take to heart the word of advice from Garrison (1985): *When using a system of standard stars, it should be obvious that the standards should be taken under the same conditions as the unknowns, but some astronomers still violate this basic rule.*

More than 600 pages of expert information and qualified guidance on standardisation is available in the Proceedings of a standardisation workshop organized in 2006; see Sterken (2007). We also refer to the discussion of the LBVs AG and η Car, and of the B[e] supergiant Hen-S22 in the paper by Sterken (see p. 139).

2. Standardisation: the Cause and the Cure

2.1. *Detector linearity*

Virtually all photometrists who graduated after 1975 never received any training in the exposure and the darkroom handling of astronomical photographic plates. Hence, most users of a photographic plate archive have only very partial knowledge of the intricacies

of the so-called *characteristic curve*, or the relation between plate density and the amount of incident light that caused the photographic grains to blacken. That curve has three distinctive parts: the *toe*, the *straight line*, and the *shoulder*. A widely used analytical form is the Honeycutt-Chaldu function, see Tsubaki & Engvold (1975):

$$log(I/I_0) = Q_1 + Q_2 D + Q_3 ln(exp(Q_5 D^{Q_6}) - 1) + Q_4 exp(Q_5 D^{Q_7}),$$

where I are the known intensities of the calibration images, I_0 a scale factor, D the measured calibration densities, and Q_i the parameters to be determined by a least-squares fit to the calibration data. This function represents well all parts of the characteristic curve; Q_2 corrects the slope of the linear part, Q_3 determines the shape of the toe, Q_4 determines the shape of the shoulder, and Q_1 shifts the curve along the axis of log I; see Liu *et al.* (1992) for typical Q-values. The flat region leftward from the toe is the *fog level*. The slope of the straight-line section of the curve is named γ and is an indication of the contrast of that emulsion. Note that this slope is wavelength-dependent. When the stellar images are underexposed, the toe will be the dominant factor in the magnitude extraction; when the images are saturated, no reliable magnitudes can be derived.

The derivation of the parameters of the characteristic curve is a painstaking task, and requires the availability of calibration spots for every batch of plates, or of calibration sequences of standard stars on each plate. The parameters of any solution are strongly dependent on the plate emulsion. Laycock *et al.* (2010), for example, bypass the characteristic curve altogether and calibrate instrumental magnitudes extracted from the plates directly via a non-linear fitted function (using a background annulus around each source) against a catalogue of known magnitudes. This magnitude extraction is a critical step, as it involves subtraction of widely different object and background densities that relate to, respectively, linear and non-linear response regimes of the characteristic curve. The same problem also applies to defocused images that are easily handled by a linear detector, but cause problems for the non-linear photographic emulsion. The use of calibration spots to calibrate the plate suffers from another problem: since the exposure of the spots (in the same or in a separate spectrograph with different light paths and optics) does not happen simultaneously with the exposure of the image, the exposure times are much shorter, implying different speed requirements for the light-sensitive material.

The method just described has led to conflicting results in the analysis of different sets of plates of the same object. An interesting case is outlined in a comparison of vintage-plate photometry of KIC 8462852 given by Schaefer (2016), and also the discussion related to Fig. 7 in Hippke *et al.* (2017). One analysis concludes that the light curves show systematic dimmings over a century-long timebase, whereas the other data-reduction approach implies that there are no such secular trends in the data.

The stellar-calibration method may fail in the case of cometary photography, where magnitude extraction of trailed stellar images adds a complication. The most severe calibration problem occurs for photometry of bright stars (like η Car) embedded in a nebula, and where the majority of historical photographs have been taken for studies of the nebula rather than for stellar photometry. As it happens, the most useful plates for such photometry are most often the underexposed 'bad' plates.

An additional element of calibration is the removal of geometrical vignetting, and the correction for variations in the sensitivity of the emulsion across the plate.

Users of vintage plates should be aware that the logbooks – if available at all – quite often do not mention the plate emulsion. A quick inspection of the plate archive at SAAO reveals that at least two dozen different emulsions had been used, but very few records identified the emulsion type in question – nor of the type of 'baking' (hypersensitisation) that may have been employed.

https://doi.org/10.1017/S1743921318002752 Published online by Cambridge University Press

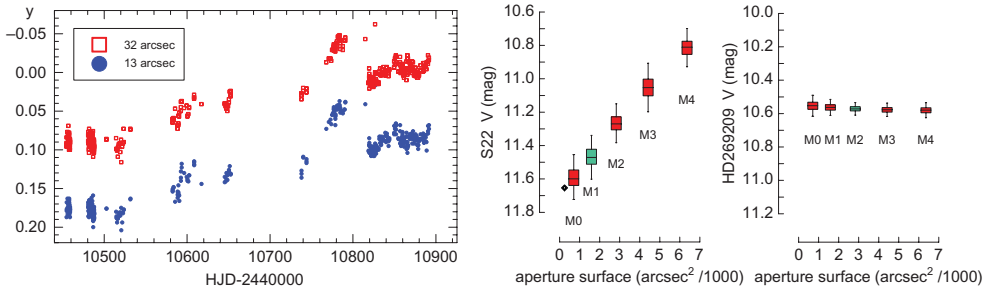

Figure 1. *Left*: CCD-based y magnitudes for η Car for two apertures. *Right:* box-whisker plots of S 22 and HD 269209 for ASAS magnitude columns as a function of aperture surface. The aperture suggested by the ASAS software (MAG_1 for S 22, MAG_2 for HD 269209) is indicated. $\diamond$ is the extrapolated ASAS V for a diaphragm of 18″ diameter. (*Reproduced from Sterken (2011), with kind permission*).

Detector saturation may occur with almost any type of detector; the effect on a photographic emulsion is less obvious, but overexposure of a CCD detector will reveal some typical 'bleeding' of overflowing pixel-well capacities into adjacent pixels. There is, though, a level of exposure that does not lead to blooming, yet causes a non-linear response when the overcharge is such that it leads to flat-topped star profiles. A good example is the high-amplitude SX-Phoenicis star CY Aqr ($P = 1\overset{\mathrm{h}}{.}46$, amplitude $0\overset{\mathrm{m}}{.}7$), which rises so fast to maximum (almost 1 magnitude in 15 minutes) that optimal CCD exposure becomes a real challenge near maximum light. Saturation then leads to a divergence in the times of maximum up to several minutes – that is, of the order of the residuals in an $O - C$ diagram, as can be seen Fig. 1 of Sterken (2010).

2.2. *Detector resolution and the point-spread function*

Both AG Car and η Car are brighter than visual magnitude 7, and are surrounded by an ejection nebula. The nebula is an additional cause for concern when combining magnitudes and colours on a century-long time-line.

Detector resolution is usually expressed in arcseconds per pixel. The best detector, from the point of view of resolution, is the photographic emulsion: black-and-white film with grain sizes of $\sim 10\,\mu$m were commonly used in mid-20$^{\mathrm{th}}$-century astrophotography, but coarser emulsions were used in the earlier days of celestial photography. With photographic images the plate or film resolution is the first limiting factor, but is overruled on the one hand by the resolution of the scanner hardware, and on the other hand by the operational resolution set by the software (including the bit depth in which the image is saved). Hence we have always to consider the combined resolution of the emulsion, scanner and detector. Good-quality commercial flat-bed scanners can allow reliable extraction of magnitudes and colours, i.e., within the calibration errors discussed in Section 2.1.

It is often not well understood that the photomultiplier tube (PMT) is basically a 1-pixel camera; the Fabry lens in the photometer, by design, smears out the light onto one spot on the photocathode surface. The detector resolution is then entirely determined by the photometer's diaphragm in the focal plane. That aperture removes the wings of the point-spread function (PSF) so that it becomes spherically symmetric (in fact, a cylinder). For that reason, it is not good practice to change the mechanical diaphragm during an observing session, unless care is taken that all standard star observations are also made with the same aperture. For stars like η Car, the difference between using a 17″ and a 35″ photometer diaphragm can amount to $0\overset{\mathrm{m}}{.}2$ in magnitude and $0\overset{\mathrm{m}}{.}02$ in

https://doi.org/10.1017/S1743921318002752 Published online by Cambridge University Press

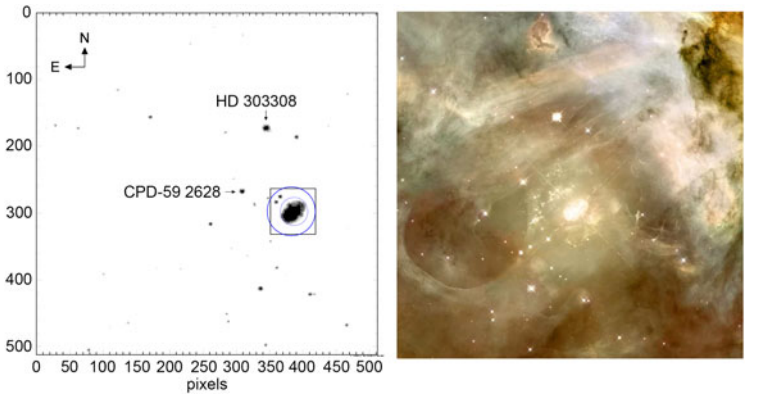

Figure 2. *Left*: 3.′5 by 3.′5 field of η Car (Strömgren y band) as described in Sterken *et al.* (1999). The small circular aperture centered on the star has a diameter of 17″, the large eccentric circular aperture has a diameter of 30″, and the square around η Car represents one pixel (28″) of a BRITE image. CPD −59 2628 is an eclipsing binary studied by Freyhammer *et al.* (2001) and HD 303308 is a constant star. The two small stellar images inside the square are Tr 16-64 and Tr 16-65. *Right*: same angular-size mosaic of the Carina Nebula assembled from frames taken with HST/ACS through an Hα filter. (*Credit: NASA, ESA and The Hubble Heritage Team.*)

colour on the standard system. Even neglecting the difference between using a 17″ and a 16″ – as used by van Genderen *et al.* (1994) – leads to a systematic error.

The hardwired diaphragm appears, in principle, only to be a problem in PMT photometry and seems not to be a problem in CCD photometry. This is not really true, because an aperture size is often recommended by the data base, or an aperture must be decided by the user. Figure 1 illustrates the trend of CCD-based Strömgren y magnitudes for η Car for two apertures, and also displays box-whisker plots for the V magnitudes of S 22 and nearby HD 269209 for ASAS-3 magnitudes as a function of aperture surface. Box-whisker plots display data by showing the minimum of a sample, the lower quartile (which cuts off the lowest 25% of the data), the median, the upper quartile, and the highest data point, without any assumption of the underlying statistical distribution of the data. The graph shows that, whereas the standard deviation of the average V magnitudes in the four apertures is $0\overset{\mathrm{m}}{.}01$ for HD 269209, it amounts to $\sigma = 0\overset{\mathrm{m}}{.}24$ for S 22. Moreover, a strong trend of brightening with aperture surface is present. The $\diamond$ is the extrapolated ASAS V (linear fit M_3 to M_0) for a photometer diaphragm of 18″ diameter.

We acquired CCD photometry of η Car spanning more than 30 years, using several telescope/detector combinations at ESO La Silla and at SAAO that had very similar pixel scales of about 0.4″ pix^{-1}; Fig. 2 presents an inverted CCD frame of one of our η Car fields. Both circular diaphragms in Fig. 2 were employed in PMT photometry of η Car using one of the Danish simultaneous *uvby* photometers at ESO, the smaller one in autocentring mode, the larger one for manually-centred operation. The larger aperture was placed off-center to make sure that the PSFs of the two faint stars are entirely inside the diaphragm, but that entailed systematic colour offsets of the order of several $0\overset{\mathrm{m}}{.}01$.

η Car was also monitored by the BRITE constellation, a nanosatellite with a 3-cm telescope aperture, a pixel resolution of ∼28″ pix^{-1} and a PSF (of the defocused images) of 8 × 8 pixels (Richardson *et al.* 2018). As such, the BRITE-Constellation R-band PSF fills about the entire field depicted on the left of Fig. 2, and includes all stars and nebular matter. One of the stars within the PSF is the eclipsing binary CPD −59 2628; it has a 1.47-day period and $0\overset{\mathrm{m}}{.}6$-deep primary eclipses. The right panel of Fig. 2 is a mosaic of the Carina Nebula obtained with HST/ACS and WFPC2, and illustrates

https://doi.org/10.1017/S1743921318002752 Published online by Cambridge University Press

the contaminants that contribute to any large-PSF magnitude extraction (especially in the R band that includes Hα). This contamination also occurs in the visual domain shortward of the R band; Herschel (1847) already described his visual observations of *that singular lemniscate-oval vacuity* – the Keyhole Nebula adjacent to η Car. It is evident that combining visual and R-band magnitudes from visual, photographic and photoelectric ground- and space-based observations of η Car – truly the most difficult galactic stellar object to be measured in a photometric standard system – is just impossible.

2.3. *Data reduction and analysis techniques*

2.3.1. Period analysis

One specific aspect of 'calibration' in time-domain astronomy is the combination of modern computer-aided methods of data analysis with vintage graphical approaches. A most important example is period determination. In earlier times, graphical methods were applied for deriving a period from a light-curve or a radial-velocity curve – two periods, at most, were sometimes extracted. Now it is straightforward to carry out Fourier analysis yielding multiple frequencies, and the results are then compared with what was obtained decades ago. The real danger here is that any systematic effects, such as shifts between data sets, will create spurious frequencies when Fourier methods are applied. Moreover, one not seldomly meets a fundamental stumbling block: the light curves are usually not available in published (hand-drawn) graphs, or the data are simply not public.

2.3.2. Transformation equations

Grmek (1981) defines 'methodological illusions' as *the extension of an idea beyond its range of validity by transforming a partially sound rule of limited application into an illusory general rule.* Examples abound in the design of early photometric systems, where linearity in the transformation equations is based on truncated Maclaurin series expansions for stars with rather uncomplicated spectral distributions. Such simple approaches are routinely applied to stars with extended atmospheres such as AG and η Car, or Hen-S22 with its curtain of emission lines. A similar condition applies to comets; cometary photometry is different from stellar photometry in the sense that the primary limitation of accuracy is not the detector, but the handling of sky-background, the choice of standard stars (which have to be changed along the path of the moving comet), extinction determination, magnitude-extraction algorithms, etc. The measurements are frequently collected at high air masses and often occur in twilight, when sky brightness changes rapidly and when few standard stars can be observed. In addition, two totally different classes of standard stars are required: G-type standard stars similar to the Sun (for determining accurately the continuum due to the reflectance of the cometary dust), and standard stars for absolute flux calibration of the emission features, for which B stars are usually chosen because of their few spectral lines. Calibrated photometry of comets cannot be achieved on the fly; telescope-camera-filter-observer combinations that happen to be available are far from optimal for producing a coherent and homogeneous set of magnitudes and fluxes worthy of incorporation in a global database.

2.3.3. Data reduction packages and software pipelines

There is no doubt that sophisticated data reduction software harbours systematic flaws. The best approach to detect these weaknesses is to submit the same data set to two or more independently developed software packages. One example that was carried out is described by Tuvikene *et al.* (2007). Another essential is finding the right answer to the secular variability of KIC 8462852; see Sect. 2.1.

https://doi.org/10.1017/S1743921318002752 Published online by Cambridge University Press

2.3.4. Decorrelation and outlier removal

Decorrelation is the practice of correcting the data by 'σ-optimisation', i.e. by best-fitting an equation that combines air mass, x, y position on the sensor, seeing, detector temperature, sky reading, etc. The resulting parameters then provide minute corrections to the magnitudes. However, one must verify that (i) there is an empirical ground for including a particular observable, (ii) one is sure that the data statistics are not dominated by outliers, (iii) constant stars are still constant after decorrelation, and that (iv) the resulting parameters behave coherently over time – that is, that the assumption of correlation is valid for **all** frames in the time series to which this procedure is applied. Obviously, the scientific paper should explain all steps in the decorrelation processing.

Outliers (also called wildshot observations) should be dealt with carefully, first by inspection of the original (raw) data – for example, CCD frames should be inspected for streaks and mishaps. Then the 'control data', i.e., the calibration frames and standardisation exposures, need to be examined for the presence and distribution of outliers. Finally, the software pipeline should be verified thoroughly.

3. Conclusions

The teaching of standardisation and calibration – if not absent altogether – is one of the most deficient aspects of PhD training. And once a student becomes an established researcher, it is very difficult to convince him/her to depart from ill-designed practice. The above-mentioned problems can only be cured through intensive teaching aimed at helping the student understand standardisation, including clear-cut observing practice with full comprehension of all black-box pipeline measuring and reduction software involved.

References

Freyhammer, L. M. *et al.* 2001, *A&A*, 369, 561

Garrison, R. F. 1985, in: D. S. Hayes, L. E. Pasinetti, & A. G. Davis Philip (eds.), *Calibration of Fundamental Stellar Quantities, Proc. IAUS 111* (Springer), p. 27

Grmek, M. D. 1981, in: M. D. Grmek *et al.* (eds.), *Boston Studies in the Philosophy and History of Science* (Springer), Vol 34, p. 10

Herschel, J. F. W. 1847, *Results of astronomical observations made during the years 1834, 5, 6, 7, 8, at the Cape of Good Hope* (London: Smith, Elder & Co.), p. 38

Hippke, M., *et al.* 2017 *ApJ*, 837, 85

Laycock, S., *et al.* 2010, *AJ*, 140, 1062

Liu, Z., *et al.* 1992, in: H. T. MacGillivray & E. B. Thomson (eds.), *Digitised Optical Sky Surveys* (Kluwer), p. 193

Richardson, N. D., *et al.* 2018, *MNRAS*, 475, 5417

Schaefer, B. E. 2016, *ApJ*, 822, 34L

Sterken, C. 2007, in: *The Future of Photometric, Spectrophotometric and Polarimetric Standardization*, *ASPCS*, 364, 613

Sterken, C. 2010, in: C. Sterken, N. Samus & L. Szabados (eds.), *Variable Stars, the Galactic halo and Galaxy Formation* (SAI, Moscow), p. 125

Sterken, C. 2011, *IBVS*, 6000

Sterken, C., *et al.* 1999, *A&A*, 346, 33

Tsubaki, T., & Engvold, O. 1975, *AAS Photo-Bulletin*, 9, 17

Tuvikene, T., *et al.* 2007, in: *The Future of Photometric, Spectrophotometric and Polarimetric Standardization*, *ASPCS*, 364, 579

van Genderen, A. M., *et al.* 1994, in: C. Sterken & M. de Groot (eds.), *The Impact of Long-Term Monitoring on Variable Star Research* (Kluwer), NATO ASI Series C, 436, 19